11-30-2007

Quantum critical scaling in graphene

Daniel E. Sheehy
Ames Laboratory

Jörg Schmalian
Ames Laboratory

Recommended Citation

Sheehy, D., & Schmalian, J. (2007). Quantum critical scaling in graphene. *Physical Review Letters, 99* (22) https://doi.org/10.1103/PhysRevLett.99.226803

Quantum critical scaling in graphene

Daniel E. Sheehy* and Jörg Schmalian
Ames Lab and Department of Physics and Astronomy, Iowa State University, Ames, IA 50011
(Dated: July 19, 2007)

We show that the emergent relativistic symmetry of electrons in graphene near its quantum critical point (QCP) implies a crucial importance of the Coulomb interaction. We derive scaling laws, valid near the QCP, that dictate the nontrivial magnetic and charge response of interacting graphene. Our analysis yields numerous predictions for how the Coulomb interaction will be manifested in experimental observables such as the diamagnetic response and electronic compressibility.

Recent experimental developments have made possible the study of graphene, a single-atom thick sheet of graphite[1]. The novel electronic properties of graphene arise from the linear, cone-shaped energy-momentum dispersion of electrons at low energies. This condensed matter realization of a relativistic Dirac spectrum follows from simple models of electrons hopping on the honeycomb lattice of graphene[2], and has been confirmed by a range of experiments [3, 4, 5].

The relevant Hamiltonian is that of relativistic Coulomb-interacting fermions in two dimensions:

$$H = \sum_l v\widehat{\mathbf{p}}_l\cdot\sigma + \frac{1}{2}\sum_{l\neq l'}\frac{e^2}{\varepsilon\left|\mathbf{r}_l-\mathbf{r}_{l'}\right|}, \qquad (1)$$

with velocity $v \simeq 10^8$cm/s[3]. $\widehat{\mathbf{p}}_l = -i\hbar\nabla_{\mathbf{r}_l}$ is the momentum operator and $\sigma = (\sigma_x, \sigma_y)$ are Pauli matrices that act in the space of the two sub-lattices of the honeycomb lattice structure. There is an additional $N = 4$ fold degeneracy caused by spin and the two distinct nodes of the dispersion, with the only tunable parameter in Eq. (1) being the dielectric constant ε.

In case of the usual electron gas, the first term in Eq. (1) is $\sum_l \widehat{\mathbf{p}}_l^2/(2m)$. Then, dimensional arguments imply that the kinetic energy dominates for high electron density while the Coulomb interaction dominates at low density. The linear Dirac spectrum changes this situation. The relative importance of the potential and kinetic energy is the same for all densities and controlled by the dimensionless number $\lambda = e^2/(4\varepsilon v\hbar)$. For $\lambda \ll 1$, the Coulomb interaction is negligible. Using the above value for the electron velocity yields $\lambda \simeq 0.55/\varepsilon$, i.e. $\lambda \simeq 0.55$ for a free standing graphene film in vacuum, implying that one cannot ignore the Coulomb interaction. The role of interactions in graphene has been discussed previously [6, 7, 8, 9, 10, 11, 12, 13, 14]. However, few specific predictions for observable quantities have been made that allow for a comparison with experiment (see, however, Ref. [15]). Here, we exploit the enlarged symmetry near its quantum critical point (QCP) to deduce numerous predictions (based on scaling theory) of interacting graphene.

In this letter, we use a renormalization group (RG) approach to the Hamiltonian, Eq. (1), and analyze the magnetic and charge response of graphene as a function of temperature T, carrier density n, chemical potential μ and magnetic field B. We make specific predictions for the the compressibility $\kappa = \partial n/\partial\mu$, the diamagnetic susceptibility χ_D, the magnetic moment $M(B)$, the heat capacity C, the infrared conductivity $\sigma(\omega)$ and the density-density correlation functions $\chi_c(\mathbf{q},\omega)$. We demonstrate that interaction effects in these quantities are measurable, allowing experiments to reveal the subtle interplay of interactions and kinetic energy in a Dirac liquid. Our analysis is based on the fact that for $T = B = \mu = n = 0$, clean graphene is located at a QCP, as illustrated in Fig. 1, and its properties nearby can be obtained via crossover scaling arguments.

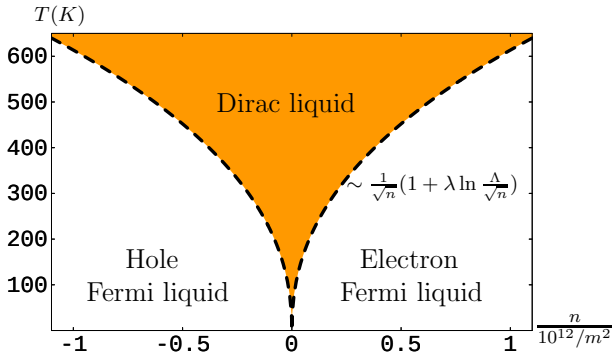

FIG. 1: (Color Online) Quantum critical phase diagram of graphene as a function of density n (in units of $10^{12}m^{-2}$) and temperature T (in K), for the vacuum case $\epsilon = 1$, showing the Dirac liquid and Fermi liquid regimes separated by the crossover temperature T^* [dashed lines, Eq. (13)], with the quantum critical point occuring at $n = T = 0$.

The low energy action that follows from Eq. (1) is

$$\mathcal{S} = \hbar\int_x \psi^\dagger\left(\partial_\tau\sigma_0 - iv\nabla_{\mathbf{r}}\cdot\sigma\right)\psi + \frac{e^2}{2\varepsilon}\int_{x,x'}\frac{n_x n_{x'}}{|\mathbf{r}-\mathbf{r}'|}. \qquad (2)$$

Here, $\psi = \psi(x)$ is a two component electron field where $x = (\mathbf{r},\tau,s)$ stands for the $2D$ position $\mathbf{r}$, imaginary time τ, and valley and spin quantum numbers $s = 1\cdots 4$, such that $\int_x \ldots = \int d^2\mathbf{r}\int_0^\beta d\tau\sum_{s=1}^4\ldots$ with $\beta^{-1} = k_{\rm B}T/\hbar$. $n_x = \psi^\dagger(x)\,\psi(x)$ is the electron density.

We perform a one-loop Kadanoff-Wilson RG analysis of Eq. (2). Fourier transforming $\psi(x)$ yields $\psi(k)$ where $k = (\mathbf{k},\omega_n,s)$ with planar wave vector $\mathbf{k}$ and Matsubara frequency $\omega_n = (2n+1)k_{\rm B}T/\hbar$. We trace out high energy

modes with $\Lambda/b < |\mathbf{k}| < \Lambda$ and obtain a renormalized action. Due to the static nature of the Coulomb interaction, the one loop fermion self energy $\Sigma(k)$ is frequency independent, i.e. the fermion dynamics remains unrenormalized: $\partial_\tau \to \partial_\tau$. Higher order diagrams[6, 10] or strong coupling effects[9] cause $\Sigma(k)$ to be ω-dependent but are beyond the leading diverging terms considered here. Similarly, vertex corrections describing interactions between electrons and collective charge fluctuations vanish. This is consistent with the Ward identity that follows from the conservation of the total charge and implies $e^2 \to e^2$ under renormalization. The only nontrivial renormalization is that of the velocity. Since $\partial\Sigma(\mathbf{k}, \omega = 0)/\partial\mathbf{k}$ diverges logarithmically as $|\mathbf{k}| \to 0$, within the RG approach this yields $v \to v(1 + \lambda \log b)$. To complete the RG procedure, we rescale the fermion field

$$\psi(\mathbf{p}, \omega, s) \to Z_\psi(b)\, \psi(b\mathbf{p}, Z_T^{-1}(b)\, \omega, s), \qquad (3)$$

with $Z_T(b) = b^{-1}(1 + \lambda \log b)$ and $Z_\psi(b) = bZ_T^{-1}(b)$ that define the relationships between fields in the original and renormalized theory. The increase of the velocity yields a decrease of the dimensionless coupling λ.

Upon iterating the RG transformation one finds the RG equations for $\lambda(b)$ as well as the temperature $T(b)$:

$$\frac{d\lambda(b)}{d\ln b} = -\lambda(b)^2, \quad \frac{dT(b)}{d\ln b} = T(b)\,(1 - \lambda(b)), \qquad (4)$$

These equations are solved by $T(b) = Z_T^{-1}(b)\, T$ and $\lambda(b) = \lambda b^{-1} Z_T^{-1}(b)$. The coupling constant is marginally irrelevant and will lead to logarithmic corrections relative to the Dirac gas of non-interacting electrons with linear spectrum. Just like in other quantum critical phenomena, the temperature is a relevant perturbation, causing crossover to a classical, finite T regime. Interactions lead to $T(b) < bT$, i.e. the quantum dynamics of the interacting Dirac liquid is more robust against thermal fluctuations than the non-interacting Dirac gas. The coupling-constant flow equation was obtained earlier in Ref. [6].

We now utilize the RG to develop general scaling relations for physical observables. We start with the electron density n and the compressibility $\kappa \equiv \partial n/\partial\mu$. A finite compressibility can be the result of a finite chemical potential μ or due to thermal excitations at $\mu = 0$. To analyze the system for finite chemical potential we add a term $-\mu \int_x \psi^\dagger \sigma_0 \psi$ to the action and rescale the fermion fields yielding $\mu(b) = Z_T^{-1}(b)\, \mu$. Upon renormalization, the number of particles per area obeys:

$$n(T, \mu, \lambda) = b^{-2} n\left(Z_T^{-1}(b)\, T, Z_T^{-1}(b)\, \mu, \lambda(b)\right). \qquad (5)$$

This equation may be written in the short-hand notation $n = b^{-2} n_R$, which we shall use henceforth, with the subscript R denoting renormalized quantities. Thus, performing the derivative with respect to μ yields for the scaling of the compressibility $\kappa = b^{-2} Z_T^{-1} \kappa_R$. As numerous similar results appear below, we now discuss the

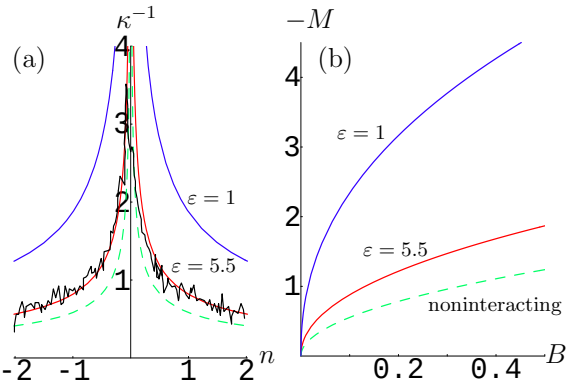

FIG. 2: (Color Online) (a) Plot of the inverse compressibility $\kappa^{-1} \equiv \frac{\partial\mu}{\partial n}$ (in units of $(10^{-10}\mathrm{meVcm}^2)$) as a function of density n (in units of $10^{12}/\mathrm{cm}^2$ for the case of $v = 10^6 m/s$ with the dielectric constant $\varepsilon = 5.5$ and $\varepsilon = 1$ (solid) and the noninteracting case (dashed), along with the data from Ref. [16]. (b) Plot of the magnetization per area (in units of μA) as a function of magnetic field (T).

physical meaning of this expression in some detail. The left side of Eq. (5) is the physical density in graphene, which is the quantity of interest. The right side is the density in the renormalized system where the effective coupling $\lambda(b)$ is *small* and the effective temperature $T(b)$ is *high*. With an appropriate, physically-motivated choice for the renormalization scale b, we can put the renormalized theory into a regime in which the calculation is particularly simple. We fix b by noting that the RG equations were derived assuming the low-T (quantum) limit, and are thus only valid for $T(b) < T_0 = D/k_\mathrm{B}$ with the bandwidth $D = \hbar v \Lambda$. Thus, we choose the renormalization condition $T(b^*) = T_0$[17] which yields $b^* = \left(1 + \lambda \log \frac{T_0}{T}\right) T_0/T$. Approximating the renormalized high temperature compressibility by its free fermion result, i.e. $\kappa_R^{-1} \simeq \pi(\hbar v)^2/(4k_\mathrm{B} T_0 \ln 2)$ we obtain

$$\kappa^{-1}(T) = \frac{\pi(\hbar v)^2}{4k_\mathrm{B} T \ln 2}\left(1 + \lambda \log \frac{T_0}{T}\right)^2, \qquad (6)$$

describing the nontrivial temperature dependence of the compressibility of graphene, valid in the shaded region of Fig. 1. Since $n(T, \mu = 0) = 0$, we can determine the density as a function of T for finite chemical potential $\mu \ll k_\mathrm{B} T$ as $n(T, \lambda, \mu) \simeq \kappa(T)\, \mu$. At $T = 0$ but finite μ we use $\mu(b^*) = \hbar v \Lambda$ and it follows in full analogy

$$n(\mu) = \frac{\mu|\mu|}{\pi(\hbar v)^2\left(1 + \lambda \log \frac{D}{|\mu|}\right)^2}, \qquad (7)$$

and $\kappa(\mu) = \partial n/\partial\mu \simeq 2n(\mu)/\mu$. Since it has recently been measured in scanning single electron transistor experiments[16] we also report the compressibility as function of density (with $n_0 = \Lambda^2/\pi$):

$$\kappa^{-1}(n) = \hbar v \sqrt{\frac{\pi}{4|n|}}\left(1 + \frac{\lambda}{2} \log \frac{n_0}{|n|}\right), \qquad (8)$$

that was also recently obtained by Hwang et al [15].

For a quantitative analysis we need to make a choice for the upper cut off. Following essentially Ref. [18] we choose Λ such that $\Lambda^2 = 2\pi/A_0$ where $A_0 = 3^{3/2}a_0^2/2$ is the area of the hexagonal unit cell with C-C distance $a_0 = 1.42 \times 10^{-10}$m. It follows $T_0 \simeq 8.34 \times 10^4$K, $D \simeq 7.24\,\mathrm{eV}$ and $n_0 \simeq 3.8 \times 10^{15}\mathrm{cm}^{-2}$. Thus, the arguments of the logarithms are very large for realistic parameters of T, μ or n, making correlation effects important.

In Fig. 2a we compare experimental data for $\kappa^{-1}(n)$ of Ref. [16] with Eq. (8) for different dielectric constants. For $\varepsilon = 5.5$, excellent agreement between theory and experiment is obtained. While the data can be fit by the Dirac gas expression $\kappa_0^{-1} = \hbar v\sqrt{\frac{\pi}{4|n|}}$ with v as a fitting parameter, it cannot be understood without incorporating interactions, since the measured velocity v is known quite accurately from other experiments. To observe the logarithmic variation of κ with n, a larger density regime or a combined T-n scaling analysis would be required.

We continue our analysis with the diamagnetic susceptibility $\chi_D = \frac{\partial M}{\partial B}$ of graphene, where B is the magnetic field and M is the magnetization per area. It was previously shown [19, 20] that, for a Dirac gas, χ_D diverges at $T = B = 0$. We will show that interactions enhance this divergence. To determine the scaling properties of χ_D, we add a gauge-field $A_\mu(x)$, to the action: $\mathcal{S} \to \mathcal{S} + \int_x A_\mu(x) j_\mu(x)$ with the electrical current $j_\mu(x) = ev\psi^\dagger(x)\sigma_\mu\psi(x)$. By repeating the RG analysis in the presence of $A_\mu(x)$, we obtain the scaling properties for the Fourier transform of the current $j_\mu(\mathbf{k},\omega) = Z_J Z_T^{-1} j_\mu(b\mathbf{k}, Z_T^{-1}\omega)$ that relates the physical current to the current in the renormalized system. The factor $Z_J = \lambda/\lambda(b)$ follows from a nontrivial vertex correction for the current operator and reflects the fact that $j_\mu(x)$ is a nontrivial composite operator (i.e., it is composed of more than one ψ field) that mixes high-and-low momentum degrees of freedom. For the diamagnetic response, we are particularly interested in $A_\mu(\mathbf{r})$ that represents a magnetic field (pointing in the $\hat{z}$ direction, normal to the graphene sheet) via $B = \hat{z}\cdot(\nabla \times \mathbf{A})$. Standard linear-response arguments dictate χ_D is related to equilibrium fluctuations of the current:

$$\chi_D = -\lim_{\mathbf{q}\to 0} \frac{1}{q_x q_y} K_{xy}(\mathbf{q}, 0), \tag{9}$$

where $K_{\alpha\beta}(\mathbf{q},\omega) = \langle j_\alpha(\mathbf{q},\omega) j_\beta(-\mathbf{q},\omega)\rangle$ is the current-current correlator. The scaling relation $K_{\alpha\beta} = Z_T K_{\alpha\beta,R}$ follows directly from that of $j_\alpha(\mathbf{k},\omega)$ yielding $\chi_D = b^2 Z_T \chi_{D,R}$, and, following the scaling analysis of κ:

$$\chi_D(T) = -\frac{e^2 v^2}{6\pi c^2 k_\mathrm{B} T}\left(1 + \lambda \log\frac{T_0}{T}\right)^2, \tag{10}$$

where we used the diamagnetic susceptibility of non-interacting Dirac fermions[20]. Thus, the RG analysis has revealed a nontrivial *enhancement* of the diamagnetic response (relative to the non-interacting result) of intrinsic graphene, a result that we have verified perturbatively to order λ, following the procedure of Ref. [21].

Our approach sheds light on the so-called universal finite-frequency conductivity[22] $\sigma(\omega)$ of graphene, related to the current-current correlator $K_{\alpha\beta}$ via the Kubo formula $\sigma(\omega) = \frac{1}{2\omega}\mathrm{Im}K^{ret.}_{\alpha\alpha}(\mathbf{q}=\mathbf{0},\omega)$, where the superscript *ret.* indicates the retarded function obtained via $i\omega_n \to \omega + i0^+$. Although $K_{\alpha\beta}(\mathbf{q},\omega)$ has nontrivial scaling behavior, the Kubo formula yields $\sigma = \sigma_R$ for $\sigma(\omega)$. This simple scaling relation is constrained by a Ward identity to be valid to *all orders* in perturbation theory, as can be shown using an argument due to Gross [23], and implies that the $T \to 0$, $\omega \to 0$ (with $\omega > T$) universal conductivity is *independent* of interactions. To see this, we take (as we have above) the perturbative result for the right side, yielding $\sigma(\omega) = \sigma(Z_T^{-1}\omega) = \frac{Ne^2}{16\hbar}$. Thus, we find that interactions do not modify the universal conductivity, in disagreement with recent results of Mishchenko [12]. Again, this result may be verified perturbatively by computing the leading-order corrections to the non-interacting universal conductivity; the crucial divergent parts of the leading diagrams identically cancel.

Our results for the scaling properties of χ_D, κ etc. can be alternatively derived from the scaling properties of the free energy energy density $F(T,\lambda,\mu,B)$. It holds $F = b^{-2} Z_T F_R$, a result that is easy to verify to leading order in perturbation theory; more generally it may be derived using the method of Ref. [24]. The scaling of the external magnetic field B follows from the scaling of the gauge field $\mathbf{A}$. Since within the RG we rescale positions via $\mathbf{r} \to \mathbf{r}' = \mathbf{r}/b$, and $\mathbf{A}$ enters via minimal coupling, we must have for the latter $\mathbf{A} \to \mathbf{A}' = b\mathbf{A}$ and therefore (from $\mathbf{B} = \nabla \times \mathbf{A}$) $B(b) = b^2 B$. This allows us to determine the scaling of the diamagnetic moment $M = Z_T M_R$, which yields at low T:

$$M(B) = -\frac{3\zeta(\frac{3}{2})}{8\pi^2}\left(\frac{2e}{c}\right)^{3/2} v\sqrt{B}\left(1 + \frac{\lambda}{2}\ln\frac{B_0}{B}\right), \tag{11}$$

plotted in Fig. 2b. Here $B_0 = \hbar/\left(2ea_0^2\right)$ is the characteristic field where scaling stops. We used the Dirac gas expression [19, 20] for the magnetization at $B(b^*) = B_0$. From the scaling behavior of the free energy, the scaling of χ_D immeadiately follows by differentiating $F(T,\lambda,\mu,B)$ twice with respect to B, while that of κ follows by differentiating twice with respect to μ. Similarly, one can easily derive scaling equations for mixed derivatives such as $\partial M/\partial\mu$ or $\partial M/\partial n$, of interest since they are measurable for two dimensional electron systems [25].

Turning to the heat capacity, we perform the derivative $C = -T\partial^2 F/\partial T^2$ and analyze the resulting scaling equation along the lines of our previous calculations. It

follows for the Dirac liquid:

$$C(T) = \frac{18T^2\zeta(3)}{\pi v^2\hbar^2\left(1+\lambda\ln\frac{T_0}{T}\right)^2}. \qquad (12)$$

The leading perturbative correction $C(T) \sim T^2 - 2\lambda T^2 \ln(T_0/T)$ fully agrees with the recent result of Vafek [11] who also argued that the dominant low-T behavior should be $C \sim T^2/\ln^2\frac{T_0}{T}$, as follows from Eq. (12). At finite density, we obtain for the linear heat capacity coefficient of the electron or hole Fermi liquid $\gamma(n) \propto \sqrt{|n|}/\left(1+\frac{\lambda}{2}\log\frac{n_0}{|n|}\right)$. Using Eq. (12) and the fact that the spin contribution of the magnetic susceptibility behaves as $\chi_s \propto c(T)/T$ implies that the magnetic response at low T is dominated by orbital effects.

Finally, we analyze the density correlation function $\chi_c(q) = \langle \delta n_q \delta n_{-q}\rangle$ where $\delta n_q = n_q - \langle n_q\rangle$. It determines the dielectric function $\varepsilon(\mathbf{q},\omega) = 1 + \frac{2\pi e^2}{\varepsilon|\mathbf{q}|}\chi(\mathbf{q},\omega)$, measurable in optical or electron energy loss scattering experiments. Due to the vanishing vertex corrections between fermions and collective charge fluctuations we find for the density $n(\mathbf{k},\omega) = Z_T^{-1} n(b\mathbf{k}, Z_T^{-1}\omega)$, yielding $\chi_c = Z_T^{-1} b^{-2}\chi_{c,R}$. If we use the random phase approximation result for $\chi_{c,R}$ at $b^*|\mathbf{q}| = \Lambda$ or $Z_T^{-1}(b^*)\,\omega = D$, we obtain $\chi_c(\mathbf{q},\omega)^{-1} = 2\pi e^2|\mathbf{q}|/\varepsilon - \Pi(\mathbf{q},\omega)^{-1}$, but with the polarization (for the Dirac liquid, see also Ref [14])

$$\Pi(\mathbf{q},\omega) = -\frac{Nq^2}{16\sqrt{(-i\omega+0^+)^2 + v^2q^2\left(1+\lambda\log x^{-1}\right)^2}}.$$

The argument of the logarithm is $x = q/\Lambda$ for $q > \frac{\omega}{\hbar v(1+\lambda\log D/\omega)}$ and $x = \omega/D$ otherwise. Despite these nontrivial renormalizations of the charge response, it follows once more that with $\sigma(\omega) = \lim_{q\to 0}\frac{\omega}{q^2}\chi_c(q,\omega)$ and the microwave conductivity of clean graphene is unaffected by interactions, as shown above.

Our results are caused by the interaction-enhanced velocity of graphene and can be rationalized by the simple substitution $v \to v^* = v\left(1+\lambda\log x^{-1}\right)$ in corresponding Dirac gas expressions, where x is proportional to the dominating scaling variable, i.e. T, $\sqrt{n}$, μ, $\sqrt{B}$, q, or ω. This insight gives an immediate physical explanation for the enhanced diamagnetism or the suppressed compressibility. The former is caused by the increased velocity of shielding currents while the latter follows from an increase in the density of states $\propto v^{-2}$. While the simple rule $v \to v^*$ is trivial to implement, we stress that it is often the result of subtle cancellations of an infinite set of divergent diagrams in the perturbation theory. To determine which scaling variable dominates for a given set of parameters we use standard crossover arguments. Consider for example temperature and density. For low density, $T(b)$ reaches its maximally allowed value T_0 before $n(b)$ reaches n_0 and $x = T/T_0$, the Dirac liquid regime of Fig. 1. The opposite happens at higher density, giving $x = \sqrt{|n|/n_0}$ in the electron and hole Fermi liquid regimes of Fig. 1. The crossover from one regime to the other takes place when $n(b^*) = n_0$ and $T(b^*) = T$ simultaneously, yielding the crossover temperature $T^*(n)$

$$T^*(n) = \frac{\hbar v}{k_B}\sqrt{\pi|n|}\left(1+\frac{\lambda}{2}\log\frac{n_0}{|n|}\right), \qquad (13)$$

which is shown in Fig. 1. Similar results can be obtained for any pair of scaling variables.

In summary, by exploiting the proximity to its QCP, we derived explicit expressions for the temperature, density and magnetic field variation of numerous observable properties of graphene. This allows a direct comparison with experiments to reveal the role of electron-electron correlations in this interacting relativistic quantum liquid.

Acknowledgments — We gratefully acknowledge useful discussions with Oskar Vafek. This research was supported by the Ames Laboratory, operated for the U.S. Department of Energy by Iowa State University under Contract No. DE-AC02-07CH11358.

* Present address: Department of Physics and Astronomy, Louisiana State University, Baton Rouge, LA 70803

[1] K.S. Novoselov, et al, Science **306**, 666 (2004).
[2] G.W. Semenoff, Phys. Rev. Lett. **53**, 2449 (1984).
[3] K.S. Novoselov, et al, Nature **438**, 197 (2005).
[4] Y. Zhang, et al, Nature **438**, 201 (2005).
[5] T. Ohta, et al, Phys. Rev. Lett. **98**, 206802 (2007).
[6] J. González, F. Guinea and M.A.H. Vozmediano, Nucl. Phys. B. **424**, 595 (1994); Phys. Rev. B **59**, R2474 (1999).
[7] E.V. Gorbar, et al, Phys. Rev. B **66**, 045108 (2002)
[8] D.V. Khveshchenko, Phys. Rev. B **74**, 161402 (2006).
[9] D.T. Son, Phys. Rev. B **75**, 235423 (2007).
[10] S. Das Sarma, E.H. Hwang and W.-K. Tse, Phys. Rev. B **75**, 121406 (2007).
[11] O. Vafek, Phys. Rev. Lett. **98**, 216401 (2007).
[12] E.G. Mishchenko, Phys. Rev. Lett. **98**, 216801 (2007).
[13] Y. Barlas, et al, Phys. Rev. Lett. **98**, 236601 (2007).
[14] R.R. Biswas, S. Sachdev, and D.T. Son, arXiv:0706.3907.
[15] E.H. Hwang, B.Y. Hu and S. Das Sarma, arXiv:cond-mat/0703499.
[16] J. Martin, et al, preprint arXiv:0705.2180.
[17] A.J. Millis, Phys. Rev. B **48**, 7183 (1993).
[18] N.M.R. Peres, F. Guinea, and A.H. Castro Neto, Phys. Rev. B **73**, 125411 (2006).
[19] A.A. Nersesyan and G.E. Vachnadze, J. Low. Temp. Phys. **77**, 293 (1989).
[20] A. Ghosal, P. Goswami, and S. Chakravarty, Phys. Rev. B **75**, 115123 (2007).
[21] M. Franz, et al, Phys. Rev. B **68**, 024508 (2003).
[22] A.W.W. Ludwig, et al, Phys. Rev. B **50**, 7526 (1994).
[23] D. Gross, in *Methods in Field Theory*, edited by R. Balian and J. Zinn-Justin (North-Holland, Les Houches, 1975).
[24] D.R. Nelson, Phys. Rev. B **11**, 3504 (1975).
[25] O. Prus, et al, Phys. Rev. B **67**, 205407 (2003).